Journal of Marine Research, 59, 453–473, 2001

Size-selective downward particle transport by cirratulid polychaetes

by David H. Shull[1,2] and Michie Yasuda[3]

ABSTRACT

The deposition of surficial sediments many centimeters below the sediment-water interface due to the reworking activities of organisms is a potentially important but easily overlooked process in marine sediments. This kind of downward particle transport is difficult to observe in the laboratory or in the field but it has important consequences for bioturbation rates and sediment geochemistry. It is also much more likely to be size dependent than other sediment-mixing mechanisms, such as conveyor-belt feeding, and may also explain some subsurface maxima observed in sediment chemical profiles.

We examined the mechanisms behind downward particle transport in Boston Harbor. Laboratory observations indicated that a large cirratulid polychaete, *Cirriformia grandis*, collected particles (glass beads) near the sediment surface and deposited them at depth. Furthermore, particle collection by this species was size dependent. *C. grandis* preferred smaller particles in the 16- to 32-μm size range relative to larger particles.

A mathematical model was developed to simulate the feeding and burrowing mechanisms of *C. grandis* and to predict the vertical profiles of tracer particles of assorted sizes in the field. The model was tested by comparing predicted profiles with profiles of glass beads measured at the field site. These glass beads were deployed in replicated patches on the bottom of Boston Harbor. Vertical distributions of the beads after 99 d were compared to profiles predicted by the model. Good agreement between predicted and measured profiles indicated that the feeding and burrowing mechanisms of *C. grandis* were sufficient to determine observed patterns of size-dependent bioturbation rates at this site.

1. Introduction

Understanding about deposit-feeding and bioturbation mechanisms has been shaped by laboratory studies of deposit-feeding species that defecate at the sediment surface, where egested particles can be conveniently seen, collected and measured. Many deposit-feeding species transport surficial material several centimeters below the sediment surface, however, where it cannot be easily observed or quantified. For example, cirratulid

1. Environmental, Coastal and Ocean Sciences Department, University of Massachusetts, Boston, Massachusetts, 02125, U.S.A.

2. Present address: Darling Marine Center, University of Maine, Walpole, Maine, 04575, U.S.A. ***email: dshull@maine.edu***

3. Biology Department, University of Massachusetts, Boston, Massachusetts, 02125, U.S.A.

polychaetes, often the most abundant macrofaunal taxon in deep-sea (Jumars and Gallagher, 1983) and some nearshore benthic communities (George, 1964b), are surface deposit feeders that have been observed to defecate sediment at depth within their burrows (George, 1964a; Myers, 1977). Terms used to describe this process include particle subduction, reverse conveyor-belt feeding, sediment caching, hoeing, and nonlocal mixing. For simplicity, we will refer to it as downward transport.

Downward transport of particles within sediments has been observed in many areas of the ocean including intertidal and subtidal sediments and the deep sea (Dobbs and Whitlatch, 1982; Smith, 1992; Levin *et al.*, 1997; Shull, 2000). It has been attributed to the activities of many different kinds of benthic animals. Downward transport may explain subsurface peaks in sediment tracer profiles (Smith and Schafer, 1984; Smith, J. N. *et al.,* 1986; Legeleux *et al.*, 1994; Wheatcroft *et al.*, 1994; Pope *et al.*, 1996) and it may play an important role in the burial and diagenesis of organic carbon (Emerson *et al.*, 1985; Graf, 1989; Blair *et al.*, 1996; Levin *et al.*, 1997). Furthermore, Dobbs (1981) and Levin *et al.* (1997) proposed that species that mix sediment in this manner might play a keystone role in organizing soft-bottom benthic communities. Because organisms collecting particles at the sediment surface are often highly selective (Whitlatch, 1980; Jumars *et al.*, 1982; Self and Jumars, 1988), downward transport rates are likely to vary with particle characteristics such as size (Wheatcroft, 1992) or age (Smith *et al.*, 1993).

However, this process is difficult to quantify. Although researchers have identified the downward transport of particles by deposit feeders in the laboratory by using colored or x-ray-dense tracers (e.g: Dobbs and Whitlatch, 1982; Starczak *et al.*, 1996), it is difficult to determine particle transport rates when sediment is egested below the sediment surface.

In order to quantitatively link the downward transport of sediment with the reworking activities of organisms, we have used a transition-matrix particle-mixing model (Shull, 2001) to examine particle transport processes at a site in Boston Harbor inhabited by a surface deposit-feeding cirratulid polychaete, *Cirriformia grandis* (Verrill), which transports sediment in this manner. The particle transport directions and particle-size selective feeding of this polychaete were observed in the laboratory. We then used the transition-matrix model to predict the mixing rates and pathways of particle tracers in the field and the vertical distributions of assorted size classes of tracer particles deployed at the sediment surface in Boston Harbor. We tested the model predictions by comparing the predicted profiles to profiles measured at the same site.

2. Methods

a. Laboratory studies

Feeding and burrowing mechanisms of *Cirriformia grandis* were investigated in the laboratory. Divers collected three large (14.5 cm inner diameter, 60 cm long) cylindrical butyrate cores at a site near the center of Boston Harbor, just west of Peddocks Island (42°17.86' N, 70°56.34' W, 8-m depth), an area that possessed large numbers of this

species (1,400 m^{-2}). The cores were returned to the laboratory and maintained at 2°C. After one day of acclimation, 150 ml of 105- to 150-μm diameter glass beads (Jaygo, Inc.) were added to the sediment surface in each core. We observed the feeding mechanisms of *C. grandis* individuals that had constructed burrows along the clear sides of the cores. After a few weeks of observation, the water in the cores was drained. When the cores had dried, they were vertically sectioned at 1-cm intervals and the distribution of glass beads in the cores was noted.

A second laboratory experiment investigated size-selective deposit feeding by *C. grandis.* Again, large-diameter cores were collected at the study site and returned to the laboratory. After the acclimation period, 80 ml of glass beads mixed with 0.2 to 0.3 g Tetramin™ fish food were added to the surface of the sediment in the cores. In two of the cores a range of bead sizes, from 1 to 250 μm in diameter, were added to the sediment surface from a beaker as a slurry. After the beads were deposited, samples of them were collected from the same region of the sediment surface where *C. grandis* feeding appendages were visible using a pipette. The collected beads were saved for later measurement. Animals were allowed to feed on the sediment and bead mixtures for 2 h. Then, the cores were sieved over 2-mm mesh and the retained *C. grandis* were fixed in 20% formalin. Samples were later transferred to 70% ethanol.

Random subsamples of the pipetted surface bead mixtures were created by settling the mixtures onto glass microscope slides following the procedures of Laws (1983). Samples were poured into a 1000-ml beaker filled with distilled water, mixed vigorously, and then allowed to settle for 12 h. Water was siphoned off and slides were dried with a heat lamp. This procedure produces randomly strewn slides (Moore, 1973; Laws, 1983). The beads were then measured using a compound microscope fitted with an ocular micrometer. Digestive tracts of *C. grandis* collected from the cores were carefully dissected after washing the animals in distilled water. The anterior 2 cm of digestive tracts from three individuals were combined and dissolved in aqua regia. The dissolved samples were evaporated to dryness, re-hydrated with dilute HCl, and the gut contents were then deposited onto microscope slides by the settling technique. The size distribution of glass beads was determined by counting and measuring the beads at 125 x.

b. Field experiments

Field experiments were conducted at the same study site. The purpose was to test the particle-mixing model by deploying glass beads of assorted sizes and then following the vertical redistribution of those beads in the sediment. On July 15, 1997, divers deployed mixtures of glass beads with diameters ranging from 1 to 250 μm (Jaygo Inc., specific gravity = 2.4) at the study site in Boston Harbor. The beads were spread within 60- by 60-cm experimental plots.

The beads were deployed in a slurry of chilled seawater by inverting a 450-ml jar, filled with beads and covered at the mouth by 0.5-mm mesh, over each plot. After approximately one hour, divers collected samples from each plot using 5.5-cm diameter butyrate cores.

Two core samples were collected from each plot. One core was collected to enumerate benthic infauna. The second core was collected to determine the vertical distribution of glass beads.

Cores were returned to the laboratory and the faunal cores were immediately sectioned at 1, 5, and 10 cm. Sections were immediately fixed in 10% buffered formalin. Later, they were transferred to 70% ethanol using a 250-μm-mesh sieve. All organisms from each depth interval were sorted and identified to the lowest feasible taxon.

Glass-bead cores were cut into 0.5-cm thick sections to 4 cm, 1-cm thick sections to 10 cm, 2-cm thick sections to 16 cm, and at 20 cm. During sectioning, approximately 3 to 5 mm of sediment around the perimeter of each section was trimmed to prevent contamination due to potential smearing of sediment and beads along the inner core wall. The remaining sample from each section was placed into a pre-weighed plastic jar. The sections were weighed wet, dried at 70°C for 24 hours, and re-weighed to determine sediment porosity.

Dried sediment samples containing the glass beads were chemically treated to facilitate counting. Large aggregates were gently broken up using a mortar and pestle. The samples were then wetted, 30% hydrogen peroxide was added, and the samples were heated in a 60°C oven. Samples were then sonicated for 5 min. Samples were then heated in 8N HNO_3, followed by further sonication. This treatment destroyed pellets, tubes, and other aggregates, and oxidized much of the organic matter in the samples. Pretests demonstrated that these procedures had no effect on the glass beads. Samples were then wet sieved through 63-μm mesh. The <63-μm fraction was collected in a 1000-ml graduated cylinder. The fraction retained on the sieve was transferred to filter paper and dried at 60°C. The dried samples were then sieved for 15 min using nested sieves and a RO-TAP shaker into 125-250-, 63-125-, and <63-μm fractions. Material in the < 63-μm size fraction was combined with material in the 1000-ml graduated cylinder. Glass beads in the > 125-μm fraction were counted at 25 or 40x magnification (depending upon bead density) under a dissecting microscope. Glass beads in the 63- to 125-μm fraction were subsampled by quartering on a glass plate. Subsamples were then counted at 40x under the dissecting microscope.

Glass beads in the finest size fractions were subsampled by drawing aliquots from the 1000-ml graduated cylinder. The subsample size ranged from 20 to 80 μl, depending upon the volume of sediment in the cylinder. The subsamples were deposited directly into a pool of distilled water on top of glass cover slips to make a final volume of 150 μl. Cover slips were dried using a heat lamp and then placed sample-side down onto glass slides containing a mixture of ethanol and glycerin. Gas bubbles were driven out of the mixture by heating the slides on a hotplate. All beads on each slide were counted at 125 or 250x with the aid of an ocular grid and measured with an ocular micrometer. Beads with diameters as small as 16 μm were easily distinguished from bubbles and other spherical objects in the preparations.

Cores for infauna and glass beads were collected again after 99 d. Samples for infauna

were sectioned at 0.5-cm intervals to 1 cm, 1-cm intervals to 10 cm and 2-cm intervals to the bottom of the core. Samples were then fixed and counted as previously described. Three glass-bead cores were processed, counted and measured in the same manner as the initial glass-bead core.

On this same sampling date, three large-diameter cores (14.5 cm diameter, 60 cm long) were collected at the study site. These cores were returned to the laboratory and imaged using a CT scanner (Omni 4001) to determine the vertical distribution of the large organisms. The CT-scanner imaged 0.8-cm thick horizontal 'slices' of each core. The number of *C. grandis* burrows visible in each slice were counted. The vertical distribution of burrows was fitted to a cumulative normal distribution by nonlinear least-squares regression (Levenberg-Marquardt method) to determine the mean and variance in the burrow depth distributions.

After imaging each core by CT-scanning, the cores were wet sieved through 1-mm mesh using filtered seawater. Retained animals were fixed in 10% buffered formalin. After transferring the samples to 70% ethanol using a 1-mm mesh sieve, the large organisms were sorted from the samples with the aid of a hand lens. These organisms were counted, identified to species, and their body weights were determined after drying at 70°C.

Also on the final sampling date, a core was collected and analyzed for organic carbon and sediment porosity. Organic-carbon content of dried and powdered sediment samples was determined using a Perkin-Elmer model 2400 CHN elemental analyzer. Prior to combustion, inorganic carbon was eliminated by adding 1M HCl to each sample according to the wet acidification procedure of Hedges and Stern (1984). The organic-matter content of the sediment (used in Cammen's [1980] ingestion-rate model) was estimated as twice the organic-carbon content (Christman and Gjessing, 1983).

c. Statistical methods

Analytical errors for the glass-bead counts included counting error and subsampling error. The counting error for the two largest size classes was determined by counting five samples containing different numbers of beads. Each of these samples was counted five times to determine the counting error as a function of sample size. For the two smaller size classes, seven slides were counted. Each slide was counted five times.

Subsampling error for the largest size fraction was not calculated because that size fraction was not subsampled before counting. Subsampling errors for each of the samples of the smaller size fractions were determined by counting a minimum of five replicate subsamples.

Effects of feeding by *C. grandis* on glass bead profiles were examined in two ways. First, results of the laboratory feeding experiment were used to determine the order of relative preference of *C. grandis* for different-sized beads. The order of preference found in the laboratory study was used when testing the hypothesis that tracer-bead mixing in the field was size dependent. The hypothesis of no differences in mixing rate among bead size classes versus the alternative of ordered mixing rates (with respect to the order of bead

preference of *C. grandis*) was tested using Page's *L* test of ordered alternatives (Hollander and Wolfe, 1973). Page's *L* test is a distribution-free test based on rank sums. For this test, we compared mixing rates for different size classes of beads using the weighted-mean depth of tracers in each sample as a measure of mixing rate. The second manner of determining the effects of *C. grandis* on tracer profiles was to visually compare the measured profiles with profiles predicted by a transition-matrix model that simulated *C. grandis* feeding and burrowing mechanisms.

3. Transition-matrix model of particle-selective downward transport by *Cirriformia grandis*

a. Model formulation

Although a variety of processes can result in downward transport of tracers, this model includes just three: the feeding activities of *C. grandis*, burrow construction by this species, and the filling of small burrows at the sediment surface. The model simulates the collection of particles near the sediment surface and the deposition of those particles at depth. It also simulates the creation of burrows that provide space at depth to accommodate the particles transported from the surface.

Development follows the transition-matrix model of Shull (2001). Previous models that quantified bioturbation rates using matrices have been presented by Jumars *et al.* (1981), Foster (1985), Boudreau (1997) and Trauth (1998). The five depth boxes in Figure 1a represent stratigraphic layers in the sediment of thickness Δx. The burial state represents permanent removal of tracer from the mixed layer. The arrows represent particle (or tracer) trajectories. The rates of movement among states are determined by transition probabilities. The transition probabilities are equivalent to the fraction of tracer moved from one box to another in one time step. For example, f_{14} represents the fraction of tracer in box 1 (at the sediment surface) moved to box 4 by downward mixing. The burrow construction terms, b_{45} and b_{43} represent the construction of burrows large enough to accommodate the incoming sediment. The advection terms, a_i, represent the downward movement of a tracer in the sediment column due to sedimentation from the water column and deposition or collection of particles by organisms. Finally, s_i represents the fraction of tracer in each box that does not move to another box. These processes are quantified by use of a transition matrix, P (Fig. 1b). This formulation allows particles to be deposited at depth due to the feeding of *C. grandis*, with the accompanied transport of sediment to create burrow space to accommodate the deposited material.

The transport probabilities in the matrix P are directly related to the feeding and burrowing activities of *C. grandis*. Let r_i be the rate (mg particle time^{-1}) at which *C. grandis* collects particles at the surface and deposits them at depth i. For boxes of unit area, the box volume is Δx. The fraction of material moved from the sediment surface to depth in one model time step, Δt, is

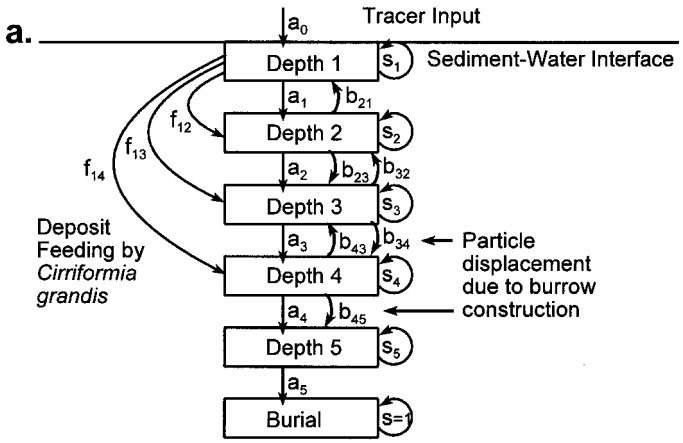

b.

State at time t ↓	1	2	3	4	5	Burial
1	s_1	$a_1 + f_{12}$	f_{13}	f_{14}	0	0
2	b_{21}	s_2	$a_2 + b_{23}$	0	0	0
3	0	b_{32}	s_3	$a_3 + b_{34}$	0	0
4	0	0	b_{43}	s_4	$a_4 + b_{45}$	0
5	0	0	0	0	s_5	a_5
Burial	0	0	0	0	0	1

State at time t + 1

Figure 1. (a) Transition-matrix model of bioturbation by *C. grandis*. Boxes represent depths in the sediment and burial. Arrows represent hypothetical tracer particle trajectories. Tracer movement is determined by the nondimensional variables, *f, a, s,* and *b,* which correspond to locations in the transition matrix (Fig. 1b). These variables represent the transition probabilities, or equivalently, the fraction of tracer in each box which moves to another box in one model time step. (b) Transition matrix. Elements of the transition matrix determine the rates of movement from box to box in the model. The elements of the main diagonal represent the fraction of tracer not moving each time step.

$$f_i = \frac{r_i \Delta t}{\Delta x \rho (1 - \varphi)}, \tag{1}$$

where φ is the sediment porosity (cm^3 pore water cm^{-3} wet sediment) and ρ is the solids density (mg particle cm^{-3} particle), so that $\rho\ (1 - \varphi)$ has units mg particle cm^{-3} wet sediment. If only a portion of particles in the sediment are selected, the fraction of selected material moved is

$$f_i^* = \alpha f_i, \tag{2}$$

where α represents particle selection (fraction tracer selected/fraction tracer available).

Assuming that burrows are completely filled with sediment collected at the surface, the

vertical components of particle movement due to burrow construction can then be determined by mass balance:

$$b_{i,i+1} = b_{i,i-1} = \frac{1}{2} f_i. \tag{3}$$

This equation states that as sediment is deposited at depth *i,* burrows are created by the upward and downward displacement of an equal volume of sediment to adjacent depths.

Movement of particles within the sediment column and sedimentation of particles from the water column result in the burial of sediment by advection. During burial, sediment is compacted as pore water is squeezed out. These processes are included in the advection term, a_i.

$$a_i = a_{i-1}\frac{(1-\varphi_{i-1})}{(1-\varphi_i)} + \frac{\sum_{j=1}^{m} f_{j,i}(1-\varphi_j)}{(1-\varphi_i)} - \sum_{j=1}^{m} f_{i,j}, \tag{4}$$

where m is the number of depth strata in the model. This equation represents a mass balance. The advection rate at any point in the sediment column is due to a balance between delivery of material to that depth (from the depth above it or from other depths due to biological transport processes) and removal of sediment due to biological transport. At the sediment-water interface, the rate of sedimentation from the water column and the biological collection and deposition of material at the sediment surface determine the advection rate.

The fraction of tracer remaining in a box after time Δt, s_i, is 1-$p_{i,+}$, where $p_{i,+}$ denotes the sum of the ith row of the transition matrix P. Because burial represents permanent removal from the mixed layer, the fraction of tracer remaining in the burial state after each time step is one (Fig. 1b). The solution to the transition-matrix model given an initial tracer profile, C_0, is $C_t = C_0 P^t$, where C_t represents the predicted tracer profile at time t.

b. Determination of model parameters from field data

Given data on the particle reworking rates of organisms at the study site and sediment porosity, all the other model parameters can be calculated. Particle reworking at the site was assumed to be due to deposit feeding and burrow construction by *C. grandis* and the passive filling of the tubes of amphipods and other tube-dwelling infauna. The feeding rate of *C. grandis* was calculated using Cammen's (1980) empirical ingestion rate formula based on the dry weights of individual organisms and sediment organic-matter content. Based on laboratory observations, it was assumed that *C. grandis* collected all particles between the sediment surface and a depth of two cm. Based on the observed distribution of feeding appendages (Fig. 2), it was also assumed that the number of particles collected in the feeding zone decreased linearly from the surface to a depth of two centimeters.

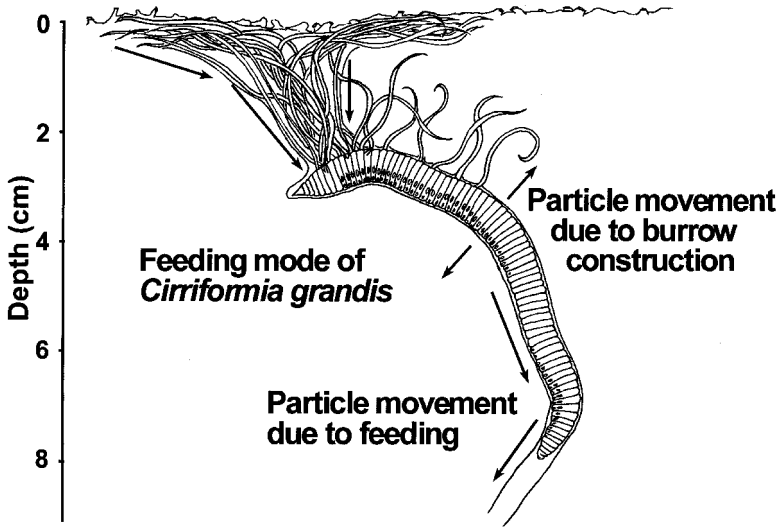

Figure 2. Feeding and burrowing mechanisms of *C. grandis*. Particles are collected near the sediment-water interface and are deposited along the entire length of the burrow. Burrows are created by displacing sediment approximately one half body width.

Collected particles were then deposited uniformly along the entire length of the tube. Tube bottoms were modeled as being normally distributed with depth. The filling of amphipod and other numerous tubes found at the sediment surface was assumed to occur rapidly relative to downward transport by *C. grandis*. Thus, the filling of these tubes determined the initial tracer distribution (sampled one hour after bead deployment) and the initial condition of the model, C_0. The appropriate model depth and time steps were determined by running the model with successively smaller values of Δx and Δt. The model box size, Δx, was set to 2 mm. The time step, Δt, was set to one day.

4. Results

a. Laboratory feeding studies

In the first laboratory study, *C. grandis* were observed to feed on beads within the top two centimeters of the sediment and defecate them at depth. Individuals that burrowed along the clear walls of the cores could be seen extending feeding tentacles within the sediment and onto the sediment surface and filling their tubes with defecated beads (Fig. 2). Burrows were created as *C. grandis* moved forward through the sediment, pushing sediment aside with its body. After sectioning the cores, beads were observed packed within the *C. grandis* burrows. In the top 2 centimeters of the cores, beads were also found within and around amphipod tubes.

Bead sizes in the sediment and in *C. grandis* digestive tracts from the second laboratory experiment were fitted to a lognormal distribution (Fig. 3). *C. grandis*

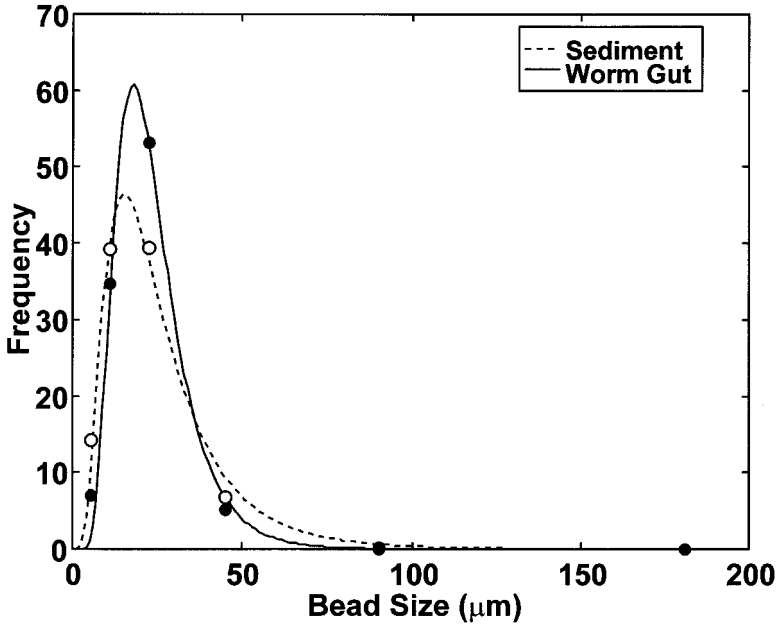

Figure 3. The frequency of beads in surface sediments during the laboratory feeding experiment and the frequency found in the digestive tracts of *C. grandis*. Experimental data were fitted to a log-normal distribution function, $f = n_1 e^{\ln(x/n_2)/n_3}$, where n_1, n_2, and n_3 were fitted parameters. Number of beads counted for surficial sediment plot was 746; for the digestive tract, 1233 beads were counted (from 3 worms).

preferentially fed on beads in the 16-32 μm range of diameters. Modeled bead distributions were used to calculate the ratio of selected versus available beads for each size class. The ratios ranged from approximately 1.4 for the 16- to 32-μm size class, to 0.014 for the 125- to 250-μm size class (Table 1).

Table 1. Summary statistics for the selection experiment and the tracer profiles for each size class. The rank sum of the depth-weighted means (t_i) was used to calculate Page's L-test statistics. The null hypothesis was $t_1 \leq t_2 \leq t_3 \leq t_4$. The alternative was $t_1 > t_2 > t_3 > t_4$.

Tracer-Bead Size Classes (μm):	16–32	33–62	63–125	126–250
Selectivity Coefficient Alpha (Fraction Consumed/Fraction Available):	1.38	0.63	0.089	0.014
Weighted-Mean Depth of Tracer Beads				
Initial Profile:	1.01	1.07	0.82	0.75
Profiles after 99 d				
Core 1:	7.23	7.26	2.20	1.34
Core 2:	4.81	2.83	2.26	2.20
Core 3:	9.96	4.36	2.53	0.92
Rank Sum of Weighted-mean Depth of Beads after 99 d (for Page's L Test):	11	10	6	3

b. Infaunal abundances and vertical distributions

The benthic community was dominated by a dense assemblage of amphipods that included the species *Ampelisca abdita*, *Ampelisca vadorum*, *Leptocheirus pinguis, Phoxocephalus holbolli, Crassicorophium bonelli, Unicola irrorata,* and *Photis pollex.* These amphipods were concentrated in the top 2 cm of the sediment. The weighted-mean depth of amphipods was 0.6 cm (± 0.5, 95% C. I.). The areal abundance of the amphipods in October 1997 was 40,000 m^{-2} (± 40,000, 95% C. I.).

Cirriformia grandis was the most abundant large deposit-feeding species at the site. Abundances were 1,400 m^{-2} (± 1000, 95% C. I.). Individual dry weights averaged 27 mg (± 3, 95% C. I.). Their vertical distributions were determined from the CT-scan images (Fig. 4). The mean depth of burrows was approximately 10 cm. The number of burrows visible in the CT-scan images decreased over the depth range of 5 to 15 cm (Fig. 5). Additional taxa at the site included oligochaetes (62,000 m^{-2}, ± 52,000, 95% C. I.), *Polydora cornuta* (1000 m^{-2}, ± 1,000, 95% C. I.), *Aricidea catherinae* (5,000 m^{-2}, ± 4,600, 95% C. I.), *Lumbrineris tenuis* (400 m^{-2}, ± 500, 95% C. I.), and several species of small bivalves (1,500 m^{-2}, ± 2,000, 95% C. I.).

c. Bulk sediment properties

Organic carbon content increased with depth from a minimum of 2.5% at the sediment surface to 3.2% at 17 cm (Fig. 6a). Porosity varied from 84% at the sediment surface to a minium of 74% at 10 cm. It then increased again to 81% at a depth of 20 cm (Fig. 6b).

d. Glass-bead profiles

The initial bead distributions were concentrated in the top one cm (Fig. 7). The weighted mean depth of the tracers was approximately the same as the weighted mean depth of amphipods, ranging from 0.75 cm for the 125- to 250-μm size class to 1 cm for the 32- to 63-μm size class (Table 1). After 99 d, the beads were mixed throughout the top 20 cm of the sediment (Fig. 8). There is a clear indication that smaller beads were mixed more rapidly than the larger ones. Bead concentrations for the smallest size (16 to 32 μm) class tended to be lowest at the sediment surface and increased with depth to at least 5 cm. Bead concentrations for the larger size classes tended to be highest near the surface. However, in cores C2 and C3 (Fig. 8) their concentrations decreased in the top 1 cm.

Differences in mixing rates across size classes were examined by comparing mean penetration depths for the four bead sizes. The alternative hypothesis was that the mixing rate should be highest for those beads preferentially selected by *C. grandis* as determined in the laboratory study (Table 1). The null hypothesis of equal weighted-mean depth for the four size classes of beads was rejected by Page's L test of ordered alternatives (Table 1, $L = 89, p = 0.001$).

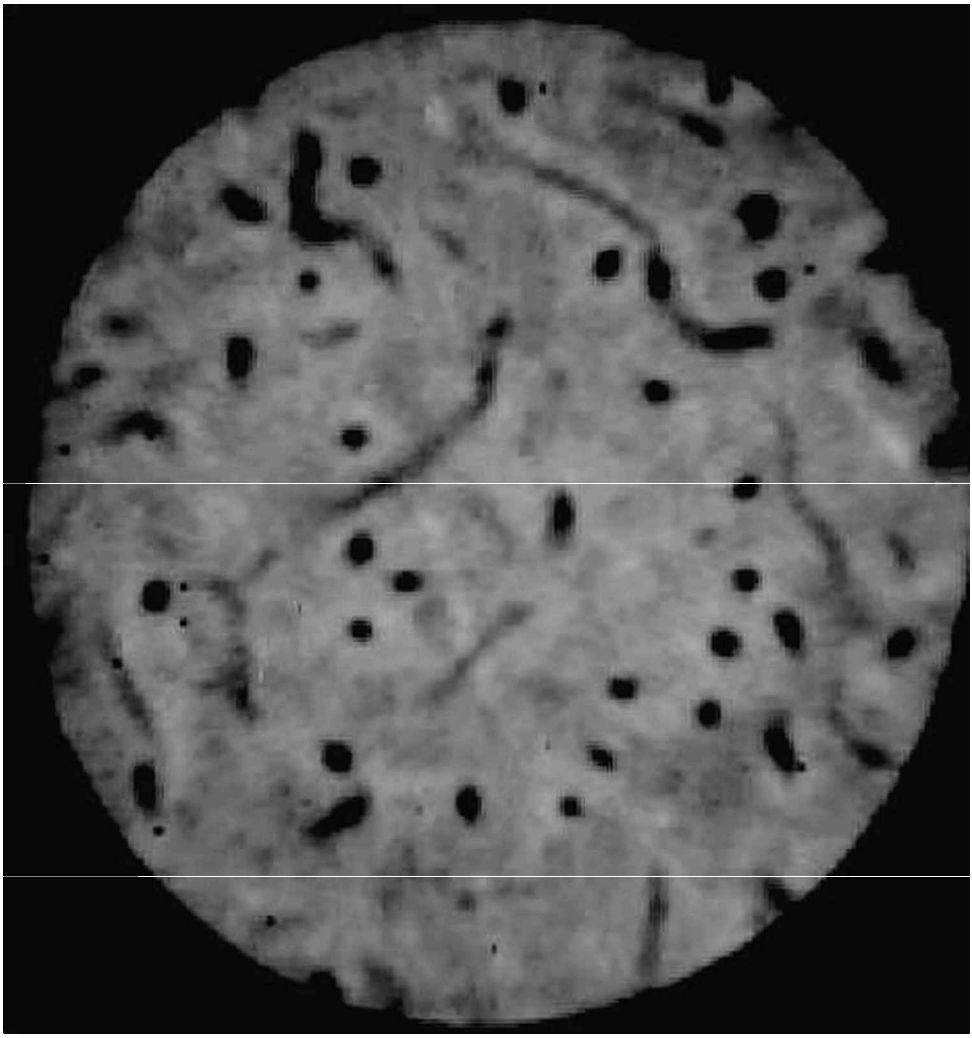

Figure 4. A CT slice through a large core at 8 cm depth. Burrows of *C. grandis* are visible. Core diameter is 14.5 cm.

e. Transition-matrix model results

The transition-matrix model was used to predict the distributions of tracers at the study site. The initial condition, C_0, was determined by the initial measured bead profile collected approximately 1 h after bead deployment. It was assumed that subsequent transport was due to deposit feeding by *C. grandis*. The model allowed *C. grandis* to collect material near the sediment surface and deposit it at depth (Fig. 9). At depth, burrow-building activities also transported sediment. The model predicted very different profiles for hypothetical tracers that were preferred compared to those that were not favored (Fig. 10). The predicted profiles for preferred beads possessed a subsurface maximum in concentration whereas

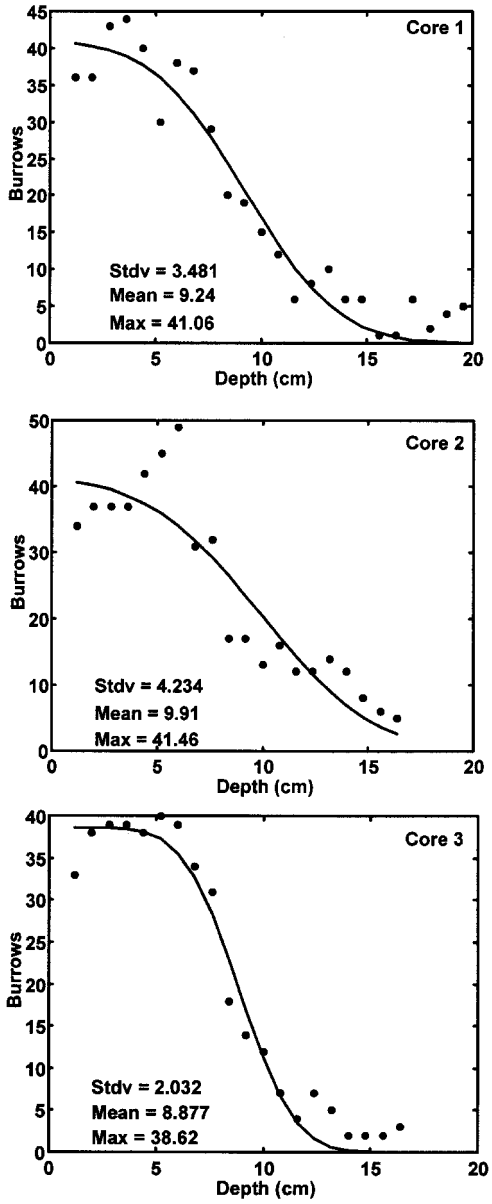

Figure 5. Vertical distribution of burrows from the CT-scans. Fitted lines represent the number of visible burrows, N, fitted to a cumulative normal distribution with mean μ and standard deviation σ, $N/2\ erfc(\ (z - \mu)/(\sqrt{2}\sigma)\ )$.

less-favored beads possessed a maximum at the sediment surface. Despite high spatial variability in measured bead distributions, tracer distributions predicted at 99 d using the measured alpha values (Table 1) for the four bead size classes corresponded reasonably

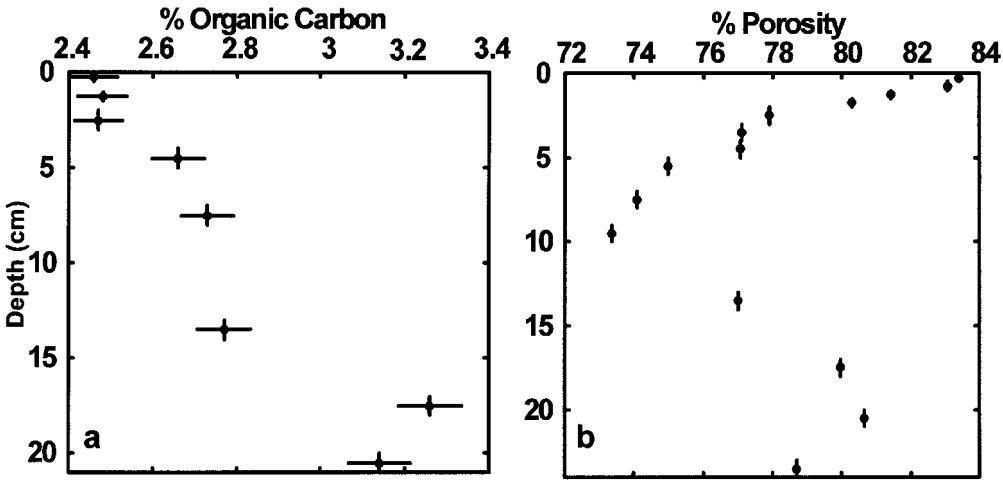

Figure 6. (a) Sediment organic carbon profile. (b) Sediment porosity. Horizontal error bars represent analytical error (± 1 s.d.), based on three replicate samples.

well to the vertical profiles of beads averaged across all three plots (Fig. 11). Model profiles deviated somewhat from measured profiles at the sediment surface where a reduction of bead numbers was observed in two cores, which was not predicted by the model. Also, the measured 16- 32-μm bead concentration at 7 cm deviated from the predicted concentrations. However, in general, the model accurately predicted the measured vertical profiles of tracers. With the exception of a few data points, model profiles matched measured profiles within the spatial variability in mixing rates at the site.

5. Discussion

A large number of downward mixing mechanisms have been identified, such as the passive filling of abandoned (or occupied) burrows (Aller and Aller, 1986; Smith, J. N. *et*

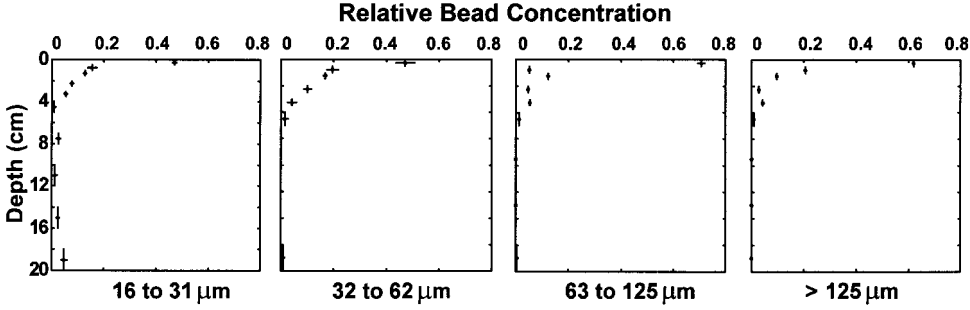

Figure 7. Initial profiles for four size classes of beads (one hour after deployment). Relative bead concentrations are normalized by the total inventory. Horizontal error bars represent analytical error (standard error, $n = 4$).

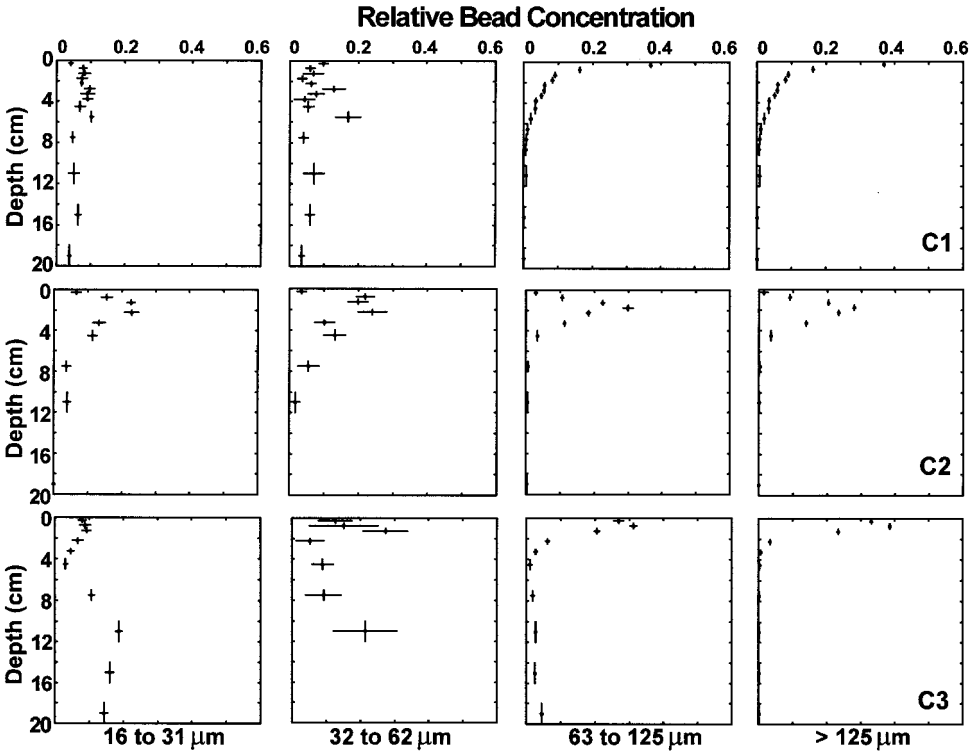

Figure 8. Profiles for four size classes of beads, 99 d after deployment. Horizontal error bars represent analytical error (standard error, $n = 4$). Each row of profiles represents bead distributions in three plots; C1, C2, and C3.

al., 1986), hoeing of surficial material by maldanid polychaetes (Dobbs and Whitlatch, 1982; Levin *et al.*, 1997), and egestion of surficial material into tubes by surface deposit feeders (Schafer, 1972; Myers, 1977). Passive filling of burrows has been modeled by a 'regeneration' model (Gardner *et al.*, 1987) and a 'nonlocal exchange' model (Boudreau, 1997) in which sediment is removed at depth to create the burrows that are subsequently filled with surficial sediment. Hoeing of surficial sediment into burrows has been modeled using the transition-matrix bioturbation model (Shull, 2001) in which subsurface deposit feeders create space at the bottom of their tubes by sediment ingestion. This space is then filled with surficial sediment by hoeing. All three of these modeling approaches include both the subsurface deposition of surface sediment, and a process for creating space at depth to accommodate this material. The creation of space at depth is not explicitly included in all models of downward mixing (e.g. Smith, J. N. *et al.*, 1986) but seems essential. The sensitivity analysis of a related model (Shull, 2001) indicated that the upward transport of sediment was as important as the downward mixing of surficial material in determining the rate of tracer burial in Narrangansett Bay. In the transition-matrix model of mixing by *C. grandis*, this process was explicitly included.

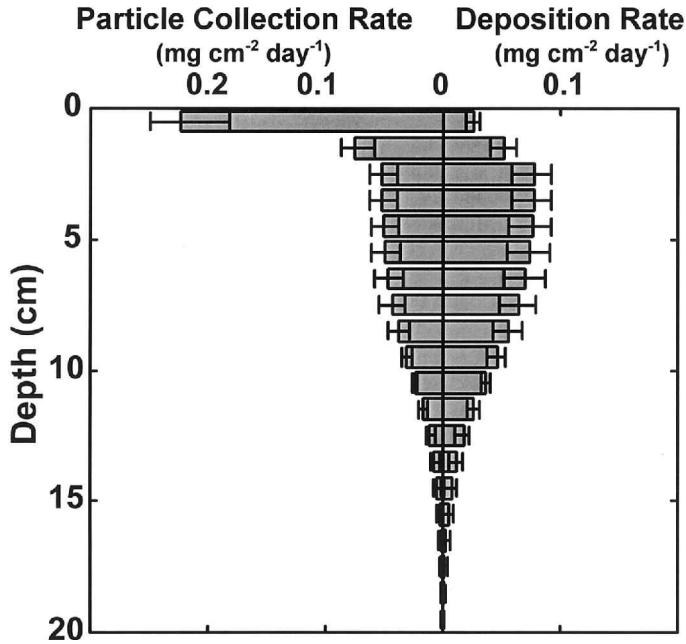

Figure 9. Modeled rates and depths of particle mixing by *C. grandis*. Particle collection and deposition rates at each depth represent the sum of all deposit-feeding rates and particle movement during burrow construction. Collection rates represent the sum of particle movement in each row of the transition matrix ($f_{i,+}$), whereas deposition rates represent the sum of particle movement in each column of the transition matrix ($f_{+,j}$). For this plot, the model box size (Δx) was set at 1 cm. Error bars represent the range of particle collection and deposition rates for each depth (from three replicate cores).

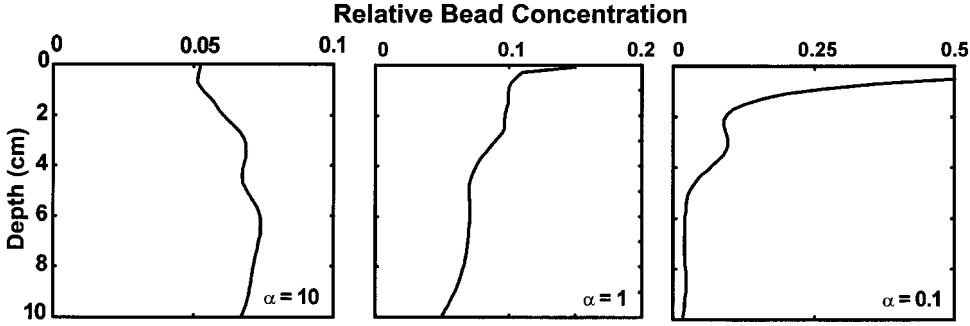

Figure 10. Predicted distribution of beads after 99 d assuming selection coefficients (α) ranging from 0.1 to 10. Bold, solid lines represent the predicted mean relative concentration profiles for each class of tracer.

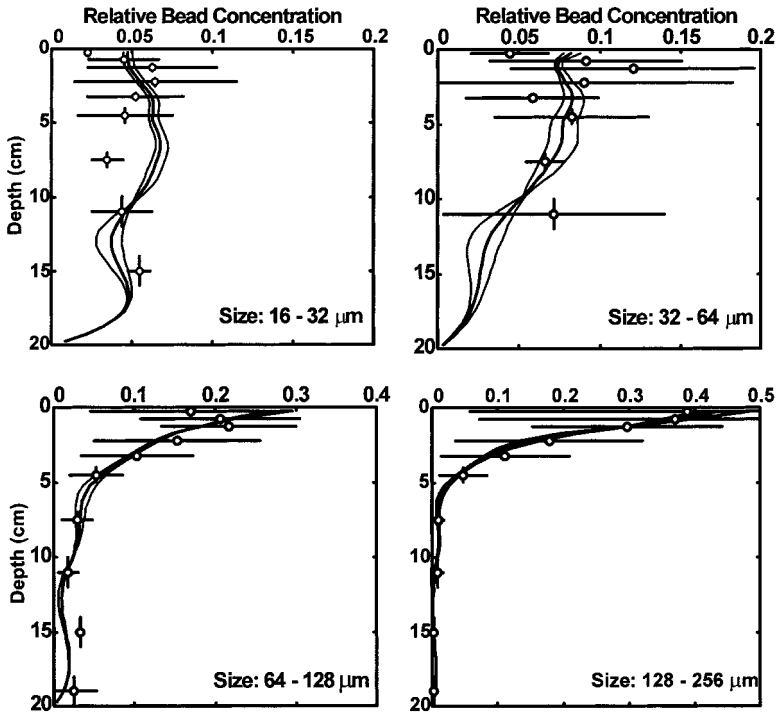

Figure 11. Predicted and measured profiles of tracer beads. Bold, solid lines represent the predicted mean concentration profiles. Finer lines represent the range of bead concentrations, given spatial variability in the abundance, vertical distribution and feeding rate of *C. grandis*. The alpha values used in the model for each bead size class are listed in Table 1. Solid circles represent average measured bead concentrations for the plots. Horizontal error bars represent one standard deviation ($n = 3$).

This model allowed size-dependent mixing to be examined. Laboratory studies indicated that *C. grandis* preferred particles in the 16- 32-μm size range. This is approximately the same range of particles that Whitlatch (1980) found were most abundant relative to other particle sizes in the digestive tracts of the related cirratulid polychaetes, *Tharyx acutus* and *Chaetozone setosa*. Effects of particle selection on tracer profiles were dramatic. Both predicted and measured profiles showed a sub-surface maximum in bead concentration for preferred bead sizes and a surface maximum for less-preferred size classes. The preferred size classes of beads penetrated the sediment much farther than less-preferred size classes. The concentration of larger beads at the sediment surface is analogous to layers of coarse particles observed in the feeding zone of conveyor-belt feeders (Rhoads and Stanley, 1965). The subsurface maximum in organic carbon at this site can also be explained by selective downward particle transport.

Size-dependent particle mixing rates have been observed previously in the field. The data of Ruddiman *et al.* (1980), as re-analyzed by Wheatcroft and Jumars (1987), indicated

that fine particles of ash were mixed more rapidly than coarser size fractions in deep-sea sediments. Wheatcroft (1992) found more rapid mixing of smaller size-classes of glass beads in the sediments of the Santa Catalina Basin. On the other hand, Whitlatch (unpublished) observed more rapid mixing of larger size classes of beads in the Panama basin. The differences between these two studies may be due to differences in mixing mechanisms occurring at the two sites (Wheatcroft, 1992). Wheatcroft *et al.* (1994) also found more rapid mixing of smaller tracer particles in Massachusetts Bay. In these previous studies, the mechanism producing size-dependent mixing was not explicitly linked to the feeding mechanisms of any species inhabiting these study sites. However, the results of this study indicate that selective feeding and downward transport by the cirratulid polychaete, *C. grandis* caused the observed profiles in Boston Harbor.

Two lines of evidence indicate that reworking by *C. grandis* produced the size-dependent mixing of the tracers. First, the order of preference of glass beads selected by *C. grandis* was the same as the relative order of mixing rates for those size classes. Second, the reasonable agreement between tracer profiles predicted by the mixing model and measured profiles indicated that downward transport by the cirratulid polychaete *C. grandis* was sufficient to determine the size-dependent particle-mixing rates at the study site. It is possible that the size-dependent mixing observed by Wheatcroft (1992) was due to the same process. Cirratulid polychaetes are very common in the deep sea (Jumars and Gallagher, 1983) and were one of the dominant taxa at Wheatcroft's site (Jumars, 1976; Smith, C. R., *et al.*, 1986, Wheatcroft, 1992). Although some species of deep-sea cirratulids, such as the mudball-building polychaetes (e.g. Jumars, 1975; Levin and Edesa, 1997) are unlikely to transport sediment in this manner, it is possible that other species exhibit downward transport as observed in shallow-water cirratulids such as *Tharyx acutus* (Myers, 1977), *Cirriformia tentaculata* (George, 1964a), and *C. grandis.*

These findings have important implications for quantifying geochemical fluxes in sediments. Often, sediment-mixing rates are quantified by fitting a tracer profile to a biodiffusion model. Fluxes of other chemical constituents in sediments can then be calculated by applying the mixing rate to a vertical profile of the chemical species of interest. However, if downward mixing is occurring at a site, the use of a traditional diffusion model could result in flux estimates that are wrong in magnitude and in direction. For example, if a diffusion model were applied to the concentration profiles with subsurface maxima such as the predicted profile in Figure 10 ($\alpha = 10$), or the profiles of glass beads in the 16- 32-μm size range (Fig 8), or to the profile of organic carbon (Fig. 6a), it would indicate an upward (down-gradient) flux. However, the tracer flux at the Boston Harbor site is downward. In coastal areas such as Boston Harbor, which are recovering from decades of pollution, fluxes of sediment-bound contaminants may be largely determined by the bioturbation rate (Olsen *et al.*, 1982; Chen, 1993). Thus, a mechanistic understanding of particle mixing is critical in order to predict the fates of contaminants and other sediment constituents in these areas.

Acknowledgments. This research benefited from the assistance of many individuals. Alex Mansfield and Peter Edwards assisted with SCUBA diving, bead deployment, and sample collection. John Healey provided transportation to and from the study site. John Outwater, Mieko Takahashi, Barbara Healy, and Carol Stuart assisted in the field. Mieko Takahashi, Alex Mansfield, YiXian Zhang, Tomohide Yasuda, and Betsy DeBlois helped process core samples on the final sampling date. Leonard Catz and Shawn Vineyard helped with the CT-scanning. The comments of Eugene Gallagher and Peter Jumars greatly improved the manuscript. Robert Chen, Ron Etter, Bernie Gardner and Gordon Wallace also provided useful comments on earlier versions of the manuscript. This research was supported by a University of Massachusetts Boston dissertation improvement grant and the University of Massachusetts Boston Craig Bollinger Memorial Award (to D.H.S.) and a grant from MIT/SeaGrant (to E. D. Gallagher). This is contribution number 01-002 from the Environmental, Coastal and Ocean Sciences Department, University of Massachusetts, Boston.

REFERENCES

Aller, J. Y. and R. C. Aller. 1986. Evidence for local enhancement of biological activity associated with tube and burrow structures in deep-sea sediments at the HEBBLE site, Western North Atlantic. Deep-Sea Res., *33,* 755–790.

Benninger, L. K., R. C. Aller, J. K. Cochran, and K. K. Turekian. 1979. Effects of biological sediment mixing on the ^{210}Pb chronology and trace metal distribution in a Long Island Sound sediment core. Earth Planet. Sci. Lett., *43,* 241–259.

Blair, N. E., L. A. Levin, D. J. DeMaster and G. Plaia. 1996. The short-term fate of fresh algal carbon in continental slope sediments. Limnol. Oceanogr., *41,* 1208–1219.

Boudreau, B. P. 1997. Diagenetic Models and Their Implementation, Springer-Verlag, 414 pp.

Cadee, G. C. 1979. Sediment reworking by the polychaete *Heteromastus filiformis* on a tidal flat in the Dutch Wadden Sea. Neth. J. Sea Res., *13,* 441–456.

Cammen, L. M. 1980. Ingestion rate: an empirical model for aquatic deposit feeders and detritivores. Oecologia, *44,* 303–310.

Chen, H-. W. 1993. Fluxes of organic pollutants from the sediments in Boston Harbor. M.S. Thesis, Massachusetts Institute of Technology, Cambridge, MA, 145 pp.

Christman, R. F. and E. T. Gjessing. 1983. Aquatic and Terrestrial Humic Materials, Ann Arbor Science, 538 pp.

Dobbs, F. C. 1981. Community ecology of a shallow subtidal sand flat with emphasis on sediment reworking by *Clymenella torquata.* M.S. Thesis, University of Connecticut, Storrs, CT, 146 pp.

Dobbs, F. C. and R. B. Whitlatch. 1982. Aspects of deposit feeding by the polychaete *Clymenella torquata.* Ophelia, *21,* 159–166.

Emerson, S., K. Fischer, C. Reimers, and D. Heggie. 1985. Organic carbon dynamics and preservation in deep-sea sediments. Deep-Sea Res., *32,* 1–21.

Foster, D. W. 1985. BIOTURB: a Fortran program to simulate the effects of bioturbation on the vertical distribution of sediment. Computers & Geosciences, *11,* 39–54.

Gardner, L. R., P. Sharma and W. S. Moore. 1987. A regeneration model for the effect of bioturbation by fiddler crabs on ^{210}Pb profiles in salt marsh sediments. J. Environ. Radioactivity, *5,* 25–36.

George, J. D. 1964a. Organic matter available to the polychaete *Cirriformia tentaculata* (Montagu) living in an intertidal mud flat. Limnol. Oceanogr. *9,* 453–455.

——— 1964b. The life history of the cirratulid worm, *Cirriformia tentaculata,* on an intertidal mudflat. J. Mar. Biol. Ass. U.K., *44,* 47–65.

Graf, G. 1989. Benthic-pelagic coupling in a deep-sea benthic community. Nature, *341,* 437–439.

Hedges, J. I. And J. H. Stern. 1984. Carbon and nitrogen determinations of carbonate-containing solids. Limnol. Oceanogr., *29,* 657–663.

Hollander, M. and D. A. Wolfe. 1973. Nonparametric Statistical Methods, Wiley, 526 pp.

Jumars, P. A. 1975. Target species for deep-sea studies in ecology, genetics, and physiology. Zool. J. Linn. Soc., *57,* 341–348.

—— 1976. Deep-sea species diversity - Does it have a characteristic scale? J. Mar. Res., *34,* 217–246.

Jumars, P. A. and E. D. Gallagher. 1983. Deep-sea community structure: Three plays on the benthic proscenium, *in* The Environment of the Deep Sea, W. G. Ernst and J. G. Morin, eds., Prentice-Hall, 217–255.

Jumars, P. A., L. M. Mayer, J. W. Deming, J. A. Baross and R. A. Wheatcroft. 1990. Deep-sea deposit-feeding strategies suggested by environmental and feeding constraints. Phil. Trans. Roy. Soc. London A, *331,* 85–101.

Jumars, P.A., A. R. M. Nowell and R. F. L. Self. 1981. A simple model of flow-sediment-organism interaction. Mar. Geol., *42***,** 155–172.

Jumars, P. A., R. F. L. Self and A. R. M. Nowell. 1982. Mechanics of particle selection by tentaculate deposit feeders. J. Exp. Mar. Biol. Ecol., *64,* 47–70.

Laws, R. A. 1983. Preparing strewn slides for quantitative microscopial analysis: A test using calibrated microspheres. Micropaleontol., *14,* 317–325.

Legeleux, F., J. -L. Reyss and S. Schmidt. 1994. Particle mixing rates in sediments of the northeast tropical Atlantic: Evidence from $^{210}Pb_{xs}$, $^{137}Cs_{xs}$, $^{228}Th_{xs}$, and $^{234}Th_{xs}$ downcore distributions. Earth Planet. Sci. Lett., *128,* 545–562.

Levin, L., N. Blair, D. DeMaster, G. Plaia, W. Fornes, C. Martin and C. Thomas. 1997. Rapid subduction of organic matter by maldanid polychaetes on the North Carolina slope. J. Mar. Res., *55,* 595–611.

Levin, L. A. and S. Edesa. 1997. The ecology of cirratulid mudballs on the Oman margin, northwest Arabian Sea. Mar. Biol., *128,* 671–678.

Moore, T. C. 1973. Method of randomly distributing grains for microscopic examination. J. Sed. Petrol., *43,* 904–906.

Myers, A.C. 1977. Sediment processing in a marine subtidal sandy bottom community. I. Physical aspects. J. Mar. Res., *35,* 609–632.

Olsen, C.R., N. H. Cutshall, and I. L. Larsen. 1982. Pollutant-particle associations and dynamics in coastal marine environments: a review. Mar. Chem., *11,* 501–533.

Pope, R. H., D. J. DeMaster, C. R. Smith and H. Seltmann, Jr. 1996. Rapid bioturbation in equatorial Pacific sediments: evidence from excess ^{234}Th measurements. Deep-Sea Res. II., *43,* 1339–1364.

Rhoads, D. C. and D. J. Stanley. 1965. Biogenic graded bedding. J. Sed. Petrol., *35,* 956–963.

Ruddiman, W. F. and others. 1980. Tests for size and shape dependency in deep-sea mixing. Sediment. Geol., *25,* 257–276.

Schäfer, W. 1972. Ecology and Paleoecology of Marine Environments, University of Chicago Press 568 pp.

Self, R. F. L. and P. A. Jumars. 1988. Cross-phyletic patterns of particle selection by deposit feeders. J. Mar. Res., 46, 119–143.

Shull, D. H. 2000. Mechanistic modeling of particle mixing in marine sediments. Ph.D. Thesis. University of Massachusetts, Boston, MA, 126 pp.

—— 2001. Transition-matrix model of bioturbation and radionuclide diagenesis. Linmol. Oceanogr., *46,* 905–916.

Smith, C. R. 1992. Factors controlling bioturbation in deep-sea sediments and their relation to models of carbon diagenesis, *in* Deep-Sea Food Chains and the Global Carbon Cycle, G. T. Rowe and V. Pariente, eds., Academic Press, 375–393.

Smith, C. R., D. J. Hoover, S. E. Doan, R. H. Pope, D. J. DeMaster, F. C. Dobbs and M. A. Altabet.

1996. Phytodetritus at the abyssal sea floor across 10° of latitude in the central equatorial Pacific. Deep-Sea Res. II., *43,* 1309–1338.

Smith, C. R., P. A. Jumars and D. J. DeMaster. 1986. *In situ* studies of megafaunal mounds indicate rapid sediment turnover and community response at the deep-sea floor. Nature, *323,* 251–253.

Smith, C. R., R. H. Pope, D. J. DeMaster and L. Magaard. 1993. Age-dependent mixing of deep-sea sediments. Geochim. Cosmochim. Acta, *57,* 1473–1488.

Smith, J. N., B. P. Boudreau and V. Noshkin. 1986. Plutonium and ^{210}Pb distributions in northeast Atlantic sediments: Subsurface anomalies caused by non-local mixing. Earth Planet. Sci. Lett., *81,* 15–28.

Smith, J. N. and C. T. Schafer. 1984. Bioturbation processes in continental slope and rise sediments delineated by Pb-210, microfossil and textural indicators. J. Mar. Res., *42,* 1117–1145.

Starczak, V. R., R. A. Wheatcroft and C. A. Butman. 1996. Particle subduction by a surface deposit-feeding polychaete worm. EOS. OS160.

Trauth, M. H. 1998. TURBO: a dynamic-probabilistic simulation to study the effects of bioturbation on paleoceanographic time series. Computers & Geosciences, *24*, 433–441.

Wheatcroft, R. A. 1992. Experimental tests for particle size-dependent bioturbation in the deep ocean. Limnol. Oceanogr., *37,* 90–104.

Wheatcroft, R. A. and P. A. Jumars. 1987. Statistical re-analysis for size dependency in deep-sea mixing. Mar. Geol., *77,* 157–163.

Wheatcroft, R. A., I. Olmez and F. X. Pink. 1994. Particle bioturbation in Massachusetts Bay: Preliminary results using a new deliberate tracer technique. J. Mar. Res., *52,* 1129–1150.

Whitlatch, R. B. 1980. Patterns of resource utilization and coexistence in marine intertidal deposit-feeding communities. J. Mar. Res., *38,* 743–765.

Received: *20 November, 2000;* revised: *2 April, 2001.*